Magnetic and spectroscopic studies of iron and manganese complexes

Tchouka, Héloïse

CHAPTER 6

Experimental Techniques

This chapter presents a brief description of the analytical techniques used for the characterization of the compounds reported in this thesis.

6.1- Elemental analysis

Elemental analysis (C, H, N,) was carried out at the Microanalytical Department of the University of Groningen, using the Euro EA Elemental Analyzer from the EuroVector Instrument and Software Company. For the analysis, approximately 5 mg of each sample was used for the determination of each element. The principle of the technique is based on thermal oxidation of the sample with Tungsten oxide (WO_3) at high temperature (1700-1800^{o}C). The gasses are further oxidized to CO_2, H_2O and N_2 and separated by GC with a "poropak QS" column at 80 ^{o}C and determined by thermal conductivity detection (TCD). The integrated peak area corresponds to the percentage content of each element in the sample.

6.2- X-Ray crystallography

X-ray crystallography is an experimental method used to determine the arrangement of atoms within a crystal.[1] When a crystal is mounted and exposed to an intense beam of monochromatic X-rays, it scatters the X-rays into a pattern of spots or *reflections* that can be observed on a screen behind the crystal. A similar pattern may be seen by shining a laser pointer at a compact disc. The relative intensities of these spots provide the information used to determine the arrangement of molecules within the crystal.

Crystals are regular arrays of atoms, and X-rays can be considered waves of electromagnetic radiation. When an X-ray strikes an electron, it produces secondary spherical waves emanating from the electron. X-ray waves are, primarily through the atoms' electrons. This phenomenon is known as elastic scattering, and the electron is known as the *scatterer*. A regular array of scatterers produces a regular array of spherical waves. These waves interfere constructively at few specific angles, determined by Bragg's law:

$$2d \sin\theta = n\lambda$$

Where d is the distance between diffracting planes, θ is the incident angle, λ is the wavelength of the beam and n is any integer. These specific angles appear as spots on the diffraction pattern called *reflections*.

A crystal with the dimensions of edges between 0.1 - 0.6 mm was mounted on top of a glass fiber and aligned on a *Bruker*[2] *SMART APEX CCD* diffractometer (Platform with full three-circle goniometer). The diffractometer was equipped with a 4K *CCD* detector set 60.0 mm from the crystal. The crystal was cooled to 100(1) K using the *Bruker KRYOFLEX* low-temperature device. Intensity measurements were performed using graphite monochromated Mo-K $\overline{\alpha}$ radiation from a sealed ceramic diffraction tube (*SIEMENS*). Generator settings were 50 KV/ 40 mA. *SMART* was used for preliminary determination of the unit cell constants and data collection control. The intensities of reflections of a hemisphere were collected by a combination of 3 sets of exposures (frames). Data integration and global cell refinement was performed with the program *SAINT,*[2] a multi-scan absorption correction was applied, based on the intensities of symmetry-related reflections measured at different angular settings (*SADABS*),[2] and reduced to F_o^2. The program suite *SAINTPLUS* was used for space group determination (*XPREP*).[2] The positional and anisotropic displacement parameters for the non-hydrogen atoms and isotropic displacement parameters for hydrogen atoms connected to the water molecules were refined on F^2 with full-matrix least-squares procedures minimizing the function $Q = \sum_h [w(\mid (F_o^2) - k(F_c^2) \mid)^2]$, where $w = 1/[\sigma^2(F_o^2) + (aP)^2 + bP]$, $P = [\max(F_o^2,0) + 2F_c^2] / 3$, F_0 and F_c are the observed and calculated structure factor amplitudes, respectively. All refinement calculations and graphics were performed on a HP XW6200 (Intel XEON 3.2 Ghz) / Debian-Linux computer at the University of Groningen with the program packages *SHELXL*[3] (least-square refinements), a locally modified version of the program *PLUTO* [3] (preparation of illustrations) and *PLATON*[4] package (checking the final results for missed symmetry with the *MISSYM* option, solvent accessible voids with the *SOLV* option, calculation of geometric data and the *ORTEP*[4] illustrations).

6.3- SQUID

SQUID (Superconducting Quantum Interference Device) is one of the most sensitive magnetometric methods. It uses a combination of superconducting materials and Josephson junctions to measure magnetic fields produced by a sample

These “magnetic atom” containing samples can display dia-, para-, ferro-, antiferro- or ferri-magnetic ordering depending upon the strength and type of magnetic interactions and external parameters such as temperature.[5]

The response of a material to a magnetic field is quantified by two parameters, *i.e.* the susceptibility χ and the permeability μ.[6] Where χ represents the variation of magnetization M, with applied field, H; $\chi = M/H$. μ is the variation of magnetic induction $B = \mu_o (H+M)$ with applied field; $\mu = B/H$.

The magnetometry data in this thesis were obtained using a Quantum Design Magnetic Property Measurement System (MPMS) equipped with a superconducting quantum interference device (SQUID) magnetometer.

Samples of between 10 and 20 mg were inserted between two pieces of cotton wool in a gel cap and were mounted within a plastic straw and connected to one end of a sample rod which is inserted into the Dewar/probe. The other end is attached to a stepper motor which is used to position the sample within the center of the SQUID pickup coils. For temperature dependent measurements, the samples were first slowly cooled to low temperature (2 K or 5 K), the field was held constant and the temperature varied from low to high values at a certain rate. The zero field cooled (ZFC) magnetization measurements were recorded in the absence of magnetic field and then the field cooled (FC) magnetizations were recorded at a constant field value. Corrections were applied for diamagnetism calculated from Pascal's constants[7]. Effective magnetic moments were calculated by the equation $\mu_{eff} = 2.828(\chi_M T)^{1/2}$, were χ_M is the magnetic susceptibility per formula unit. The inverse magnetic susceptibility data were fitted with a straight line; from the Curie-Weiss Law equation $\chi_M = C/T-\theta$. From which the Curie constant (C) and the Curie-Weiss temperature (θ) were calculated. The field dependence of magnetizations was determined by varying the applied field up to 5 T at constant temperature.

6.4- Spectroscopic methods

6.4.1- NMR (Nuclear Magnetic Resonance) spectroscopy

NMR spectroscopy requires NMR active nuclei (*e.g.,* ^{1}H, ^{13}C) of a sample at a frequency characteristic of the isotope, when the sample is placed in a magnetic field. The field dependent frequency shift corresponding to an isotope, is converted to a field-independent dimensionless value referred to as chemical shift.[8,9] Analysis of a NMR spectrum gives information on the number and type of chemically equivalent atoms in a molecule. NMR

spectra were recorded on a Varian Mercury (400 MHz) for ^{1}H. Chemical shifts are reported in ppm relative to the residual solvent peak.

6.4.2- EPR (Electron Paramagnetic Resonance) spectroscopy

EPR, also known as ESR, spectroscopy is used to characterize molecules and ions containing unpaired electrons. This technique uses microwave-induced transitions between magnetic energy levels of electrons with certain spin and orbital angular momentum.[10] In principle it is similar to that of nuclear magnetic resonance spectroscopy (NMR) except that rather than the nuclei of individual atoms; it focuses on the interaction of the unpaired electron in the molecule with an external magnetic field.

In the presence of a magnetic field, the magnetic moment of an electron, which splits into two components $m_s = +1/2$ and $m_s = -1/2$, is aligned parallel ($m_s = -1/2$) corresponding to the lower energy state or antiparallel ($m_s = +1/2$) to the field. The difference between the lower and the upper energy state is given by the equation $\Delta E = h\upsilon = g\beta B$ where B is the strength of magnetic field, h is the Planck constant, υ is the frequency of radiation, β is the Bohr magneton and g is called g-factor or Landé g-factor.[11]

EPR experiments were performed on a Bruker ER200D spectrometer equipped with an Oxford EPR-900 continuous flow cryostat. A single crystal of $(Ph_4P)_2[Fe(CN)_5im]\cdot 2H_2O$ was placed in a quartz insertion Dewar filled with liquid nitrogen and placed in the resonance cavity. The crystal was mounted on a quartz rod of a single-axis goniometer. The crystal was mounted such that one of the axes is parallel to the rotation axis being perpendicular to the external magnetic field direction and parallel to the magnetic component B of the microwave field. The external magnetic field direction in the crystal *ab* plane was chosen to be parallel to one of the axis of the $[Fe(CN)_5im]^{2-}$ complex, which is expected to be along the principal g-factor. g Values were calculated from the spectra recorded at 115 K by rotating the crystal along the *a*, *b* and *c* axes.

6.4.3- Mössbauer spectroscopy

Mössbauer spectroscopy involves using the gamma rays emitted from the nuclei of a radioactive source to probe those in the sample to be studied.

^{57}Fe Mössbauer uses a ^{57}Co source, this isotope decays by electron capture to the I = 5/2 excited state of ^{57}Fe. This excited state decays to the I = 3/2 excited state or to the I = ½ ground state by gamma-ray emission.

The source contains the parent nucleus of the Mössbauer isotope, embedded in a rigid matrix. The gamma rays emitted from this are passed through the material being investigated and those transmitted through the absorber are detected and counted. If the nuclei in the source and absorber are in equivalent environment (*i.e.* the energy of the nuclear transition is equal in both nuclei) the gamma rays will be resonant and an absorption will occur. In order to probe the energy levels in nuclei in different environments we must scan the energy of the Mössbauer gamma ray must be swept. This is achieved by moving the source relative to the absorber. The Doppler effect produces a shift in the gamma ray energy allowing it to match the energy level (gap) in the absorber.

The Mössbauer results were obtained in collaboration with the Laboratoire de Chimie de Coordination, CNRS, Toulouse, France. The spectra were collected in an exchange gas cryostat. A conventional constant acceleration spectrometer was used, equipped with a ^{57}Co/Rh source kept at RT and calibrated with Fe metal. Isomer shift values are reported relative to iron metal (α-Fe). The spectra were fitted on a PC with a least squares minimization procedure assuming Lorentzian line shapes.

6.4.4- FT-IR (Infrared) absorption spectroscopy

FT-IR absorption spectroscopy is one of the most common spectroscopic techniques used by chemists. This spectroscopic technique is used to determine the chemical functional groups in the sample. IR spectra are obtained by detecting changes in transmittance as a function of frequency. The infrared radiation region is situated between the red end of the visible region and the microwave region (13000 to 10 cm^{-1}); which is commonly divided into three regions; near IR (13000- 400 cm^{-1}), mid IR (4000-200 cm^{-1}) and far IR (200-10 cm^{-1}).

A polyatomic molecule of *n* atoms (3*n* total degrees of freedom) results in the 3*n* – 6 (for non-linear molecules) or 3*n* – 5 (for linear molecules) fundamental vibrations (also known as normal modes of vibration), some of which produce a net change in dipole moment. Since most of functional groups give rise to bands in particular regions, the IR spectrum is useful for identifying the presence of different types of bonds and thus specific functional groups of a molecule.

It is possible to make a statement about the wavenumber at which certain type of vibrations is expected to occur. For a diatomic molecule A-B, the wavenumber of the infrared radiation absorbed by a vibration can be approximated using Hooke's law (Equation 1)
Since the wavenumber of a bond according to Hooke's law, is inversely dependent on the reduced mass of the two atoms involved in the bond, it is therefore possible to deduce the wavenumber of the same system containing a different isotope.

$$\bar{\nu} = \frac{1}{2\pi c}\sqrt{\frac{k}{\mu}} \quad \text{with} \quad \frac{1}{\mu} = \frac{1}{m_A} + \frac{1}{m_B} \longrightarrow \mu = \frac{m_A \times m_B}{m_A + m_B}$$

k is the force constant for the bond

μ is the reduced mass of the A-B system

c is the speed of light

$\bar{\nu}$ is the wavenumber

Equation 1: Hooke's law

For AB and A'B bond systems with A' being an isotope of element A, assuming that both AB and A'B bonds have the same force constant, the wavenumber of the A'B ($\bar{\nu}_2$) system can be estimated from that of AB system ($\bar{\nu}_1$) as in equation 2.

$$\bar{\nu}_1 = \frac{1}{2\pi c}\sqrt{\frac{k}{\mu_1}} \qquad \text{and} \qquad \bar{\nu}_2 = \frac{1}{2\pi c}\sqrt{\frac{k}{\mu_2}}$$

$$\frac{\bar{\nu}_2}{\bar{\nu}_1} = \sqrt{\frac{\mu_1}{\mu_2}} \longrightarrow \bar{\nu}_2 = \bar{\nu}_1\sqrt{\frac{\mu_1}{\mu_2}}$$

Equation 2: Estimation of the wavenumber of isotopically substituted compound vibrational modes assuming that the force constant k is unchanged.

An illustrative example is ^{12}CN ($\bar{\nu}_1$) and its isotopologue ^{13}CN ($\bar{\nu}_2$). By considering the conditions above, the relation between the wavenumbers of both systems can estimated (Equation 3).

$$\mu = \frac{m_C \times m_N}{m_C + m_N} \qquad \mu_1 = \frac{12 \times 14}{12 + 14} = 6.46 \qquad \mu_2 = \frac{13 \times 14}{13 + 14} = 6.74$$

$$\overline{\nu}_2 = 0.979 \times \overline{\nu}_1$$

Equation 3: Estimation of the wavenumber of a ^{13}CN ($\overline{\nu}_2$) from that of ^{12}CN ($\overline{\nu}_1$). μ_1 and μ_2 are the reduced mass of ^{12}CN and ^{13}CN, respectively.

The isotope shift is the difference between $\overline{\nu}_2$ and $\overline{\nu}_1$.

FT-IR spectra of all compounds were recorded using a ZnSe/Diamond ATR attachment on a Perking-Elmer Spectrum 400 FT-IR/FT-FIR in the range between 4000 and 600 cm^{-1}.

6.4.5- Raman spectroscopy

Raman spectroscopy is based on inelastic scattering of monochromatic light. When a photon interacts with a molecule, the photon distorts the electronic cloud around the nuclei to form a non-stable virtual state. The photons are instantaneously reemitted with a frequency higher or lower or the same as incident photon. If the scattered photons have the same frequency the interaction is called elastic (Rayleigh) scattering, however if the frequency is higher than the incident photon frequency, the scattered light is called anti-Stokes radiation. The Raman scattering is called Stokes radiation when the incident photon frequency is lower than the scattered frequency.[12] The figure below shows the different scattering.

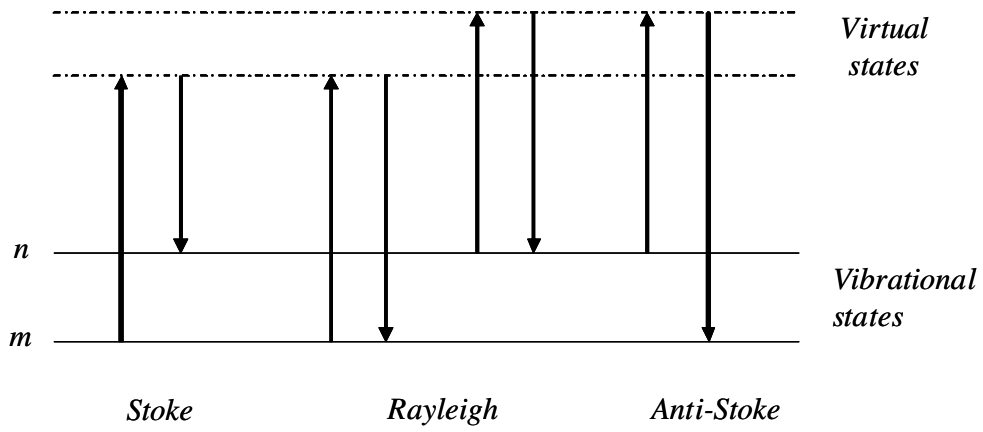

Figure 6.1: The lowest energy vibrational state m is shown at the base with states of increasing energy above it. Upward arrows are virtually absorbed energy and the scattered energies are downward arrows.

There is a basic selection rule which is required to understand Raman Spectrum. Intense Raman scattering occurs from bonds, which undergo a change in their polarizability during the vibration. Usually, symmetric vibrations undergo the largest changes and give the greatest scattering. This contrasts with infrared absorption where the absorption is caused by a change in dipole moment and hence asymmetric vibrations are the most intense. Not all vibrational structure of a molecule need to, or in some cases can, be both infrared and Raman active and the two techniques usually give quite different intensity patterns.

Raman spectra were recorded using a Perking Elmer Spectrum 400 Raman station equipped with a polarization accessory (PE) for independent polarization of excitation laser (785 nm) and the Raman backscattering or via a Olympus BX51 upright reflecting microscope coupled to the Raman station by fiber optic cables. Polarized Raman spectra were obtained by placing a U-ANT polarizer in the common excitation and Raman scattering collection pathway and orientation was varied using a U-SRG 2 circular rotable stage. The principle is based on the illumination of the sample with a laser beam and the scattered light is collected with a lens and is sent through an laser line filter and spectrophotometer to obtain the Raman spectrum on a CCD detector.

6.4.6- UV/Vis (Ultraviolet- visible) absorption spectroscopy

Visible wavelengths cover a range from approximately 400 to 800 nm and the ultraviolet region covers the region between 190-400 nm.

When ultraviolet or visible light passes through a sample, it can be absorbed. The absorbed energy must be equal to that needed to excite the molecules from the ground state to an electronically excited state (*i.e.* the resonance condition).

Some common electronic transitions are:

Transition involving *n*, σ and π electrons. For organic compounds for which the most common transitions are *n* to π∗ and π to π* (π∗ is the antibonding orbital). The other transitions are either too high in energy and so are out of the UV/Vis region (σ to σ*) or are weak (*n* to σ*).

Transitions involving charge transfer in inorganic compounds are referred to as charge-transfer absorptions in which an electron is transferred from the donor to an orbital associated to the acceptor in the complex.

The UV-Vis absorption spectrometer measures the intensity of the light passing through the sample (I, transmitted light) and compares it to the intensity of the light without the

sample (I_0 incident light). The ratio I/I_0 is called transmittance. The resulting spectrum is presented as a graph of absorbance (A) versus wavelength. The absorbance is related to the concentration of the sample through the Beer-Lamber Law.

$A = -log_{10}(I/I_0) = \varepsilon.c.L$ where L is the pathlength through the sample, and c the concentration of the absorbing species. For each species and wavelength, ε is a constant, the molar absorptivity.

The UV/Vis absorption measurements were recorded on a JASCO V630 or V570 spectrophotometer. Concentrations of 1.0 mM of compounds in water or acetonitrile and 1 cm pathlength quartz cuvettes were used. For the solid samples, diffuse reflectance spectra were recorded as solid solutions in $BaSO_4$ (spectroscopic grade) using a JASCO V570 UV/Vis/NIR spectrometer equipped with an integrating sphere. The samples were powdered and homogenously mixed with the $BaSO_4$ before being filled into the sample holder. Spectra were recorded in the range of 200 – 2500 nm.

6.4.7- MCD (Magnetic Circular Dichroism) spectroscopy

MCD as well as CD (Circular Dichroism) spectroscopies measure the differential electronic absorption of left and right handed circularly polarized light as a function of wavelength. However, in contrast to CD, MCD spectroscopy is performed in a strong magnetic field parallel to the direction of propagation of the circular polarized light. [13] Whereas CD spectroscopy is sensitive to chirality in the structure of the chromophore or its environment (induced CD); MCD spectroscopy gives information on electronic excited state properties and on ground state magnetic properties of a compound. The MCD signal is proportional to three contributions, designated as MCD A-, B- and C-terms and can be temperature or magnetic field dependent. [14,15]

The A-terms correspond to a sigmoid or derivative band shape curve and its intensity arises from a degenerate excited state of the molecule which is split by the magnetic field.

The C-term has an absorption-like band shape at low temperature and its intensity arises from a degenerate ground state which is split in the magnetic field due to the Zeeman effect. Since the degenerate ground states are typically of spin degeneracy hence, only paramagnetic compounds show C-term signals.

B-term signals have an absorption band shape and arise from the mixing of different states in the magnetic field.

A- and B-terms are temperature independent whereas the C-term is temperature dependent. MCD spectra were recorded on a Jasco J-815 CD spectrometer at 293 K using a DeSa magnet (1.4 Tesla) as cuvette holder.

6.4.8- LD (Linear Dichroism) spectroscopy

LD is a simple technique that can give information on the molecular characteristics and also information on the orientation of the chromophores in a sample such as a crystal.[16] It is based on the difference in absorption between parallel ($A_{//}$) and perpendicular ($A_{\perp}$) polarized light according to an orientation axis. From the equation $LD = A_{//} - A_{\perp}$, it is possible to determine how much energy is absorbed in one dimension of the molecule relative to the other.

If the polarization of the probed transition is *parallel* to the orientation direction, then $LD = A_{//} - A_{\perp} > 0$

If the polarization of the probed transition is *perpendicular* to the orientation direction, then $LD = A_{//} - A_{\perp} < 0$

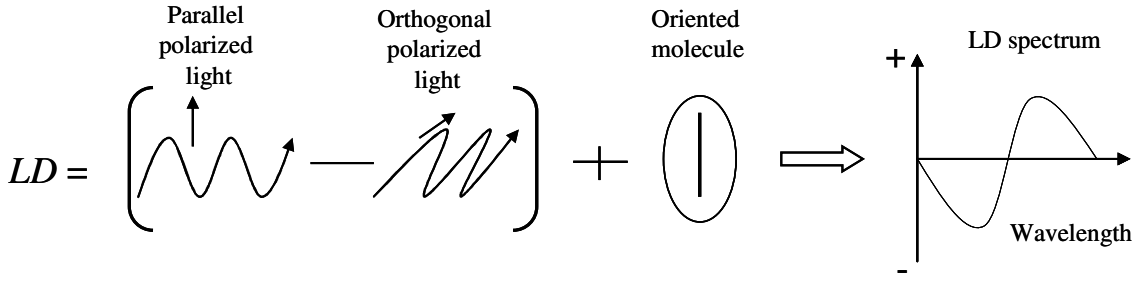

Figure 6.2: LD spectroscopy.

LD spectra were recorded on a Jasco J-815 CD spectrometer. The single crystal was mounted on a goniometer and the data were collected through 360° by increments of 15°.

6.5- Electrochemistry

6.5.1- CV (Cyclic Voltammetry)

CV is an electroanalytical technique widely used to study redox active compounds. CV is extensively used due to the ability to observe redox behavior. CV consists of measuring the

resulting current over time while varying the potential, at a controlled scan rate, of an electrode in a solution.[17] [18,19]

CVs were recorded on a Model CHI630C or Model CHI760B electrochemical workstation (CH Instruments).

1.0 mM concentration of analyte was prepared in anhydrous acetonitrile containing 0.1 M tetrabutylammonium hexafluorophosphate ($TBAPF_6$). A Teflon shrouded glassy carbon working electrode, a Pt-wire counter electrode and a SCE were used.

6.5.2- Spectroelectrochemistry

UV-Vis spectroelectrochemistry was performed in a homemade Optically Transparent Thin Layer Electrochemical (OTTLE) cell, consisting of a 2 mm quartz cuvette containing an aqueous solution of 10^{-3} M concentration of the sample and 100 mM concentration of the electrolyte (KNO_3). Pt-gauze working electrode, Pt-wire counter electrode (separated from the main solution with a fritted glass tube) and a SCE reference electrode were used.

6.6- References:

1. Atkins, P.; Overton, T.; Rourke, J.; Weller, M.; Armstrong, F., Shriver and Atkins', *Inorganic Chemistry*, 5th Eds. **2010**, 223.
2. SMART, SAINTPLUS and SADABS. Area Detector Control and Integration Software. Smart Apex Software Reference Manuals. Bruker Analytical x-ray Instruments. Inc., Madison, Wisconsin, USA., Bruker **2007**.
3. Sheldrick, G. M., *Acta Cryst* A, **2008**, *64*, 112.
4. Spek, A. L. (2008) PLATON. Program for the Automated Analysis of Molecular Geometry (A Multipurpose Crystallographic Tool) Version of Mrt. **2008**. University of Utrecht, The Netherlands, Spek, A. L., *J. Appl. Cryst.,* **2003**, *36*, 7.
5. Clarke J.; Braginski A. I., (Eds.), *The SQUID handbook*. **1**. Wiley-Vch, **2004**.
6. Drago, R. S., *Physical Methods in Inorganic Chemistry*, Reinhold Chemistry Textbook Series, Chapman and Hall Ltd., London, **1965**, 389.
7. Boudreaux, E. A.; Mulay, L. N. *Theory and Applications of Molecular Paramagnetism*, John Wiley and Sons: New York, **1976**, 491.

8. Keeler, J., *Understanding NMR Spectroscopy*. John Wiley & Sons, **2005**.

9. Hesse, M.; Meier, H.; Zeeh, B., *Spectroscopic Methods in Organic Chemistry*, Thieme **1997**, 71.

10. Drago, R. S., *Physical Methods in Inorganic Chemistry*, Reinhold Chemistry Textbook Series, Chapman and Hall Ltd., London, **1965**, 328.

11. Rieger P. H., *Electron Spin Resonance: Analysis and Interpretation*. Royal Society of Chemistry, Cambridge, UK, **2007**.

12. Smith, E.; Dent, G., *Modern Raman Spectroscopy- A Practical Approach*. John Wiley & Sons, Ltd, **2005**.

13. Stephens, P. J., Magnetic Circular Dichroism., *Ann. Rev. Phys. Chem.,* **1974**, *25*, 201.

14. Johnson, M. K., *Physical Methods in Bioinorganic Chemistry: Spectroscopy and Magnetism,* Que, L. Jr. Ed., University Science Books, **2000**, 233.

15. Oganesyan, V. S.; George, S. J.; Cheesman, M. R.; Thomson, A. J., *J. Chem. Phys.,* **1999**, *110*, 762.

16. Nordén B., Lindblom G., and Jonas I., *J. Phys. Chem.,* **1977**, *81*, 2086.

17. Kissinger, P. T.; Heineman, W. R., *J. Chem. Ed.*, **1983**, *60*, 702.

18. Mabbott, G. A., *J. Chem. Ed.*, **1983**, *60*, 697.

19. Zoski, C. G., *Handbook of Electrochemistry*. Elsevier Ed., **2007**.